Research article

PRAME promotes proliferation of multiple myeloma cells through CTMP/Akt/p21/CCND3 axis by ubiquitinating CTMP and p21

Kai Sun [a,1], Lu Yang [a,b,1], Feng Wang [c], Ying Liu [c], Nan Xu [a], Zong-Yan Shi [a], Wen-Min Chen [a], Ke Li [c], Ya-Zhen Qin [a,*]

[a] *Peking University People's Hospital, Peking University Institute of Hematology, National Clinical Research Center for Hematologic Disease, Beijing Key Laboratory of Hematopoietic Stem Cell Transplantation, Beijing, 100044, PR China*
[b] *Department of Hematology, The First Affiliated Hospital of Zhengzhou University, Zhengzhou, 450052, PR China*
[c] *Institute of Medicinal Biotechnology, Chinese Academy of Medical Sciences & Peking Union Medical College, Beijing, 100050, PR China*

A B S T R A C T

Multiple myeloma (MM) is a Ubiquitin Proteasome System (UPS)-dysfunction disease. We previously reported that high *PRAME* transcript levels associated with unfavorable progression free survival (PFS) in patients with no bortezomib therapy, and bortezomib-containing regimen significantly improved PFS in patients with high *PRAME* transcript levels, which indicated that *PRAME* expression was prognostic for MM patients, and was related to proteasome inhibitor treatment. However, molecular mechanisms underlying the above clinical performance remain unclear. In the present study, MM cell models with *PRAME* knockdown and overexpression were established, and *PRAME* was identified to play the role of promoting proliferation in MM cells. P-Akt signaling was found to be activated as *PRAME* overexpressed. As a substrate recognizing subunit (SRS) of the E3 ubiquitin ligase, PRAME targets substrate proteins and mediates their degradation. CTMP and p21 were found to be the novel targets of PRAME in the Cul2-dependent substrate recognition process. PRAME interacted with and mediated ubiquitination and degradation of CTMP and p21, which led to accumulation of *p*-Akt and CCND3 proteins, and thus promoted cell proliferation and increased bortezomib sensitivity in MM cells.

1. Introduction

Preferentially expressed antigen of melanoma (PRAME), a member of cancer-testis antigen (CTA) family, was first found in melanoma patients [1]. Aside from expression in testes and low expression in ovaries, adrenals and endometrium, PRAME was not detected in healthy human issues but expressed in various human solid and hematologic malignancies [2]. PRAME is a tumor-associated antigen (TAA) [3]. Several studies on solid tumors reported that high expression of *PRAME* was related to poor prognosis [4–6]. However, prognostic significance and biological effects of *PRAME* expression in hematologic malignancies remain controversial and insufficient.

Multiple myeloma (MM) is a kind of hematological malignancy characterized by clonal accumulation of plasma cells and monoclonal secretion of immunoglobulin or light chain proteins [7]. A large amount of protein secretion accelerates protein metabolism,

driving proteasomes in malignant plasma cells in highly active states, and thus normal proteins controlling proliferation, cell cycle, apoptosis, and DNA repair were over ubiquitinated and degraded by proteasomes, which makes the proteasome a rational candidate target for MM therapy [8,9]. Bortezomib was the first proteasome inhibitor on clinical practice [10]. Standard first-line therapy for newly diagnosed MM was proteasome inhibitor-containing chemotherapy regimens, but treatment responses varied among patients [11]. We and others reported that more than half of MM patients overexpressed *PRAME* at diagnosis [12,13]. *PRAME* overexpression at diagnosis correlated with adverse progression free survival (PFS) in patients with no bortezomib therapy, and bortezomib-receiving regimen significantly improved PFS in patients overexpressing *PRAME* [12,14], suggesting that *PRAME* expression levels might impact the prognosis of MM and might be associated with proteasome-related protein degradation process. There have been no reports about *in vivo* and *in vitro* studies to explore molecular mechanisms of the impact of PRAME on MM.

MM is a Ubiquitin Proteasome System (UPS)-dysfunction disease [7], and previous studies have revealed that PRAME made sense in UPS. Costessi et al. [15] and Wadelin et al. [16] individually used K562 and HL60 cell lines to demonstrate that PRAME functioned as a substrate recognizing subunit (SRS) of the E3 ubiquitin ligase and participated in the degradation process of intracellular proteins through UPS. Whether PRAME was also functioned as an SRS in MM and its recognized substrates remained unknown to date.

In the current study, we investigated the biological roles of *PRAME* in promoting cell proliferation, cell cycle progression, and cell migration and invasion in MM cells. Furthermore, we demonstrated that PRAME interacted with CTMP and p21, regulated their protein levels through the ubiquitination pathway, and thus promoted MM cell proliferation and increased sensitivity to bortezomib through CTMP/Akt/p21/CCND3 axis in MM cells.

2. Materials and methods

2.1. Cell culture and establishment of stable transfected cell lines

Human MM cell lines LP-1, RPMI8226, KM-3 and SKO-007 were used in this study. LP-1 and SKO-007 cell lines were purchased from the American Type Culture Collection (ATCC). RPMI8226 cell line was kindly provided by Cell Bank Shanghai Institute of Cell Biology (Shanghai, China). KM-3 cell line was conserved in our laboratory. All MM cell lines were cultured in RPMI-1640 medium (Gibco, Life Technologies, Carlsbad, CA, USA) supplemented with 10 % fetal bovine serum (Gibco), 100 U/mL penicillin, 100 mg/mL streptomycin and 2 mM L-glutamine (Gibco). The cells were grown at 37 °C in a humidified 5 % CO_2 atmosphere.

LP-1 cells were infected with lentivirus containing human *PRAME* RNA, *PRAME* shRNA lentiviral particles or corresponding blank control lentiviral particles (GeneChem, Shanghai, China). RPMI8226, KM-3 and SKO-007 cells were infected with human *PRAME* shRNA lentiviral particles or blank control lentiviral particles (GeneChem). Medium containing lentiviral particles was replaced with a complete medium after 12h of infection. Stably transfected cells were selected with 2 μg/mL puromycin dihydrochloride (GeneChem) at 96h post-infection for 2 weeks.

2.2. RNA extraction and qRT-PCR (quantitative real-time PCR)

RNA was extracted and reverse-transcribed into complementary DNA (cDNA). The *PRAME* transcript level was measured by TaqMan-based qRT-PCR technology as we described previously [17]. The *PRAME* transcript level was calculated as *PRAME* copies/*ABL* copies in percentage.

2.3. Cell proliferation viable assays

Cells were seeded into 12-well plates at a density of 1×10^4/mL. The evolution of cell number with time was followed 7 days by cell counting realized at successive time intervals of 24h. Experiments were performed in triplicate. In addition, the Cell-Light EdU Apollo643 In Vitro Kit (RioBio, Guangzhou, China) was used to measure cell proliferation according to the manufacturer's instructions.

2.4. Cell cycle analysis

Cells were seeded in 12-well plates and starved by adding serum-free medium for G1 synchronization. After 24h, complete medium was added for an additional 48h. Cells were fixed in 75 % ethanol, and stained with prodium iodide (BD Pharmingen, San Jose, CA, USA). DNA content was measured by flow cytometry (BD biosciences, San Jose, CA, USA). The data were analyzed using Modfit LT2.0 software (Coulter Electronics, Hialeah, FL, USA).

2.5. Assessment of apoptosis

Cells were seeded in 12-well plates at 37 °C in a humidified 5 % CO_2 atmosphere for 48h with or without bortezomib. Apoptotic cells were determined using the Annexin V-APC/7-AAD apoptosis kit (KeyGEN BioTECH, Suzhou, China) according to the manufacturer's instructions. Cells were immediately analyzed by flow cytometry (BD biosciences). Analysis was performed using Kaluza flow analysis software (Beckman Coulter, Brea, CA, USA).

2.6. Colony-forming assays

Cells were suspended in 1 mL of complete Methocult™ H4230 medium (STEMCELL Technologies, Vancouver, Canada) and plated in 6-well plates at a concentration of 1×10^4 cells/well. Colonies were maintained at 37 °C with 5 % CO_2 and 95 % humidity for 12 days. Colonies of ≥50 cells were counted. Assays were performed in triplicate.

2.7. Cell migration and invasion assay

Cell migration and invasion were evaluated using Transwell invasion assays with or without Matrigel (BD). 1×10^5 cells were seeded into the upper chamber of a Transwell insert (8 μm pores, Corning, NY, USA) in RPMI-1640. The upper chamber was placed into the Transwell containing a medium supplemented with 10 % FBS in the lower chamber. The cells in lower chamber were counted after 24h and experiments were done in triplicate.

2.8. Xenograft tumor model

The animal studies were approved by the Institutional Animal Care and Use Committee of Peking University People's Hospital (RDX2018-01). Male BALB/c nude mice that were 4–6 weeks old were obtained from Beijing Vital River Laboratory Animal Technology Co., Ltd. The mice were pretreated with intraperitoneal injections of cyclophosphamide once daily at 100 mg/kg for two consecutive days. Totally 10 mice were randomly divided into two groups (n = 5 in each group), and LP-1 cells transfected with human *PRAME* shRNA lentiviral particles or blank control lentiviral particles were injected subcutaneously into the right forelimb armpit. Tumor diameters were measured every 2 days until day 30. Tumor volume (mm³) was estimated by measuring the longest and shortest diameter of the tumor as described [18]. Mice were euthanized on day 30 and tumors were surgically removed for subsequent experiments.

2.9. Immunohistochemistry staining

The procedure for immunohistochemistry was the same as what Li et al. reported [19]. Briefly, tumors were fixed in 10 % neutral buffered formalin and embedded in paraffin. Four μm thick paraffin sections were baked at 68 °C for 90 min. Sections were then deparaffinized, rehydrated, antigen retrieval and quenched endogenous peroxidase. After blocking, rabbit anti-Ki-67 primary antibodies (1:200, Abcam, Cambridge, UK) were added and the slides were incubated at 4 °C overnight. After washing three times, sections were incubated for 30 min with corresponding secondary antibodies at room temperature. Signals were detected with freshly made DAB substrate solution (ZSGB-BIO Company, Beijing, China).

2.10. Label-free quantitative proteomics (Label free) technology

Total protein of RPMI8226 cells was extracted followed by ultrasonic lysis and protein quantification. After trypsin digestion, liquid chromatography-mass spectrometry analysis was performed for peptide signal capture. Mass spectrometry data was retrieved through Maxquant (v1.6.5.0) supported by Uniprot Homo_sapiens database (Hangzhou Jingjie, China).

2.11. Immunoprecipitation-mass spectrometry (IP-MS)

RPMI8226 cells were collected and lysed for 30 min on ice. Soluble lysates were incubated with anti-PRAME (ab219650, Abcam) at 4 °C overnight, followed by incubation of Protein A/G Plus-Agarose (sc2003, Santa Cruz Biotechnology, TX, USA) at 4 °C for 2 h. Immunocomplexes were eluted by Laemmli buffer and separated by SDS-PAGE. The separated gels were stained with Coomassie brilliant blue, and were cut into 6 molecular weight ranges and a heavy chain IgG band. Followed by stain removal and trypsin digestion of the cut gels, immunocomplexes were subjected to the Thermo Fisher Orbitrap Fusion Lumos Mass Spectrometer. IP-MS was assisted by Hangzhou Jingjie Biotechnology Co., Ltd (Hangzhou, China).

2.12. Immunoprecipitation and endogenous ubiquitination assay

Cell extracts were incubated with primary antibodies PRAME (ab219650, Abcam) for co-immunoprecipitation (co-IP), p21 (ab109520, Abcam) and CTMP (14692-1-AP, Proteintech, Hubei, China) for endogenous ubiquitination assay or control IgG in a rotating incubator overnight at 4 °C, followed by incubation with protein A/G Plus-Agarose (sc2003, Santa Cruz Biotechnology, TX, USA) for another 2 h. The immunoprecipitates were washed three times with lysis buffer and analyzed by immunoblotting with anti-CTMP and anti-p21 for co-IP assay, as well as anti-ubiquitin (sc8017, Santa Cruz Biotechnology, TX, USA) for ubiquitination testing.

2.13. Western blot and cycloheximide (CHX)-chase assay

Cell lysates were prepared with RIPA lysis buffer (Beyotime Biotechnology, Shanghai, China) and analyzed by immunoblotting. Anti-PRAME (ab219650, Abcam), anti-p21 (ab109520, Abcam), anti-p27 (ab32034, Abcam), anti-CDK4 (23972, Cell Signaling Technology, MA, USA), anti-Bcl-2 (12789-1-AP, Proteintech), anti-Bax (50599-2-Ig, Proteintech), anti-PARP (9532, CST), anti-

cleaved-PARP (5625, CST), anti-CTMP (14692-1-AP, Proteintech), anti-Akt (60203-2-Ig, Proteintech), anti-*p*-Akt (4060, CST), anti-CCND3 (66357-1-Ig, Proteintech) and anti-GAPDH (5174, CST) were used as primary antibodies.

For CHX-chase experiments, cells were treated with 50 μg/mL CHX (HY-12320, MedChemExpress, New Jersey, USA) in combination with 10 μmol/L MG-132 (HY-13259, MCE) or DMSO for 0, 2 h, 4 h and 8 h.

2.14. MM patients' plasma cell isolation and Micro RNA extraction

Fresh bone marrow (BM) specimens of newly diagnosed MM patients were used to extract mononuclear cells (MNCs). Plasma cells were sorted using CD138 immunomagnetic beads (Miltenyi Biotec, Bergisch Gladbach, Germany) from MNCs according to the manufacturer's instructions. RNA was then extracted from the purified plasma cells using the RNeasy Micro Kit (Qiagen, Hilden, Germany) according to the manufacturer's instructions.

2.15. Statistical analysis

All data were presented as the mean ± standard deviation (SD). The Student's *t*-test was used to determine significant differences between two groups, and one-way ANOVA was used to estimate differences between three or more groups. All *P*-values were obtained using two-tailed tests, and $P < 0.05$ was considered statistically significant. The statistical analysis was performed using SPSS software version 26.0 (SPSS, Inc., Chicago, IL) and GraphPad Prism 7 (GraphPad Software, Inc., La Jolla, CA).

3. Results

### 3.1. Construction of PRAME stable knockdown and overexpression cell models

PRAME transcript and protein levels in MM cell lines were measured by qRT-PCR and Western blot. PRAME expression levels were high in RPMI8226, KM-3, and SKO-007 (all PRAME/ABL >750 %), and were relatively low in LP-1 cells (Fig. 1A and B). Therefore, *PRAME* expression was knocked down in all four cell lines and over-expressed only in the LP-1 cell line by Lentivirus. *PRAME* transcript levels were knocked down to 18 %, 25 %, 20 % and 39 % of control in RPMI8226, LP-1, KM-3 and SKO-007 cells, respectively (Fig. 1C). In the overexpression group of LP-1, the *PRAME* transcript level was 2.5 times higher than the control group (Fig. 1C). PRAME protein level changes also identified the construction of *PRAME* stable knockdown and overexpression cell models (Fig. 1D).

3.2. PRAME promotes MM cells' proliferation

RPMI8226 and LP-1 cell lines were used for cell proliferation viable assays. The growth curve, EdU and colony formation assays indicated that *PRAME* overexpression significantly promoted cell proliferation, whereas *PRAME* knockdown slowed down cell proliferation (Fig. 2A–C). Next, a xenograft tumor model was built to investigate the role of *PRAME* on *in vivo* tumor growth. Consistent with cell assays, the tumor formation rate in the *PRAME* knockdown group was lower than that in the control group (Fig. 2D). Moreover, tumor volume (Fig. 2E) and weight (Fig. 2F) in the *PRAME* knockdown group were lower than those in the control group.
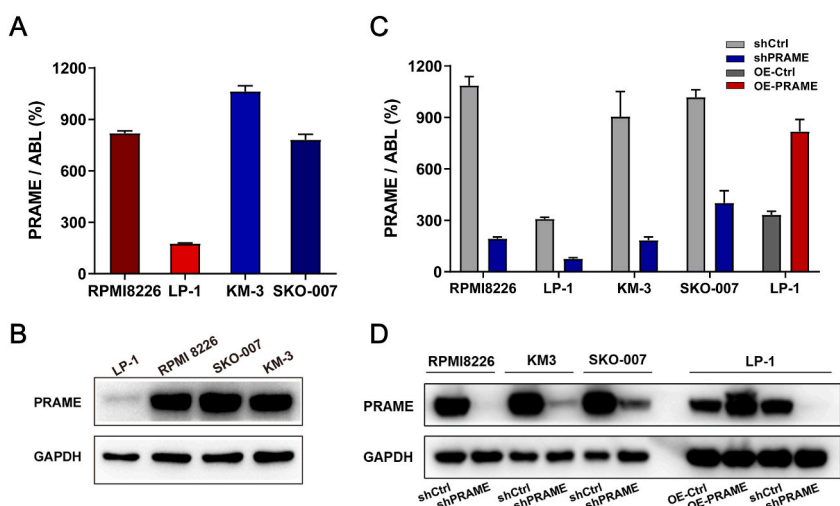
Fig. 1. PRAME expression in MM cell lines and construction of *PRAME* knockdown and overexpression cell models. PRAME expression in human MM cell lines RPMI8226, LP-1, KM-3 and SKO-007, was tested by (A) qRT-PCR and (B) Western blot (related to Fig. S2 and Fig. S3). The efficiency of PRAME knockdown and overexpression was verified by (C) qRT-PCR and (D) Western blot (related to Fig. S4 and Fig. S5). Data are the means ± SD of 3 assays in qRT-PCR assay.
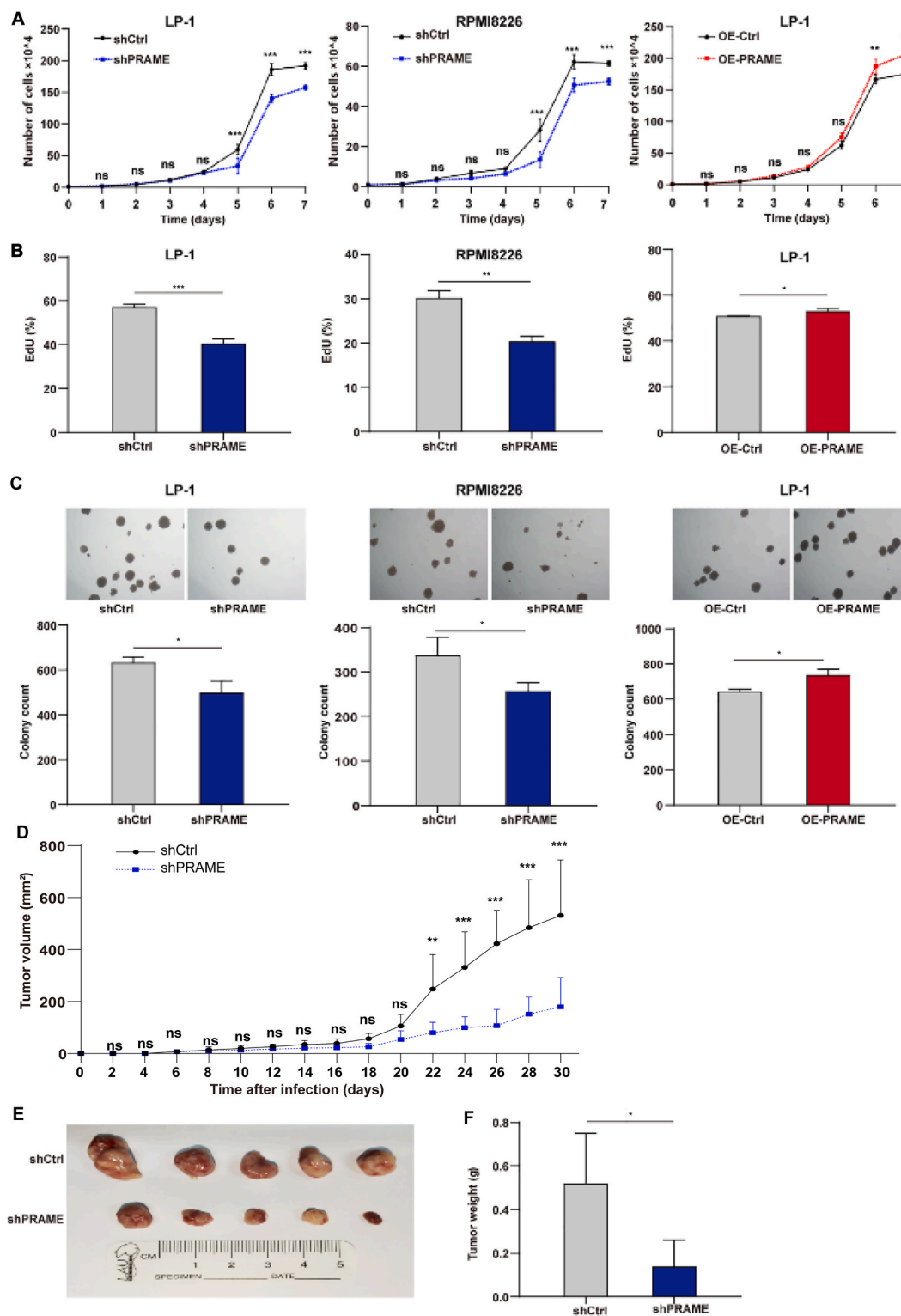
Fig. 2. *PRAME* promotes proliferation of MM cells in vitro and *in vivo*. (A) Growth curve analysis by cell count, (B) EdU assay tested by flow cytometry and (C) colony-forming assays showed that *PRAME* promoted cell proliferation. Data are the means ± SD of 3 assays. (D, E) The volume and (F) weight of LP-1-derived xenografts in the *PRAME* knockdown and control groups. ns, no significance; *$P < 0.05$; **$P < 0.01$; ***$P < 0.001$.

Taken together, these data demonstrated that *PRAME* promoted MM cells' growth.

3.3. PRAME promotes cell cycle progression, cell migration and invasion

Flow cytometry analysis demonstrated that *PRAME* knockdown in RPMI8226 and LP-1 increased the proportion of cells in G_0/G_1 phase and decreased the proportion of cells in S phase (Fig. 3A–D). Opposite results were found when *PRAME* was overexpressed in LP-1 cells (Fig. 3E and F), suggesting that *PRAME* promoted cell cycle transition from G_0/G_1 to S phase. Furthermore, the IHC results indicated that tumors of *PRAME* knockdown group expressed less Ki67 than those of the control group (Fig. 3G and H). In addition, *PRAME* knockdown group cells showed an obvious reduction in the migratory (Figs. S1A–C) and invasive (Figs. S1D–F) ability. *PRAME* overexpression showed the opposite results.
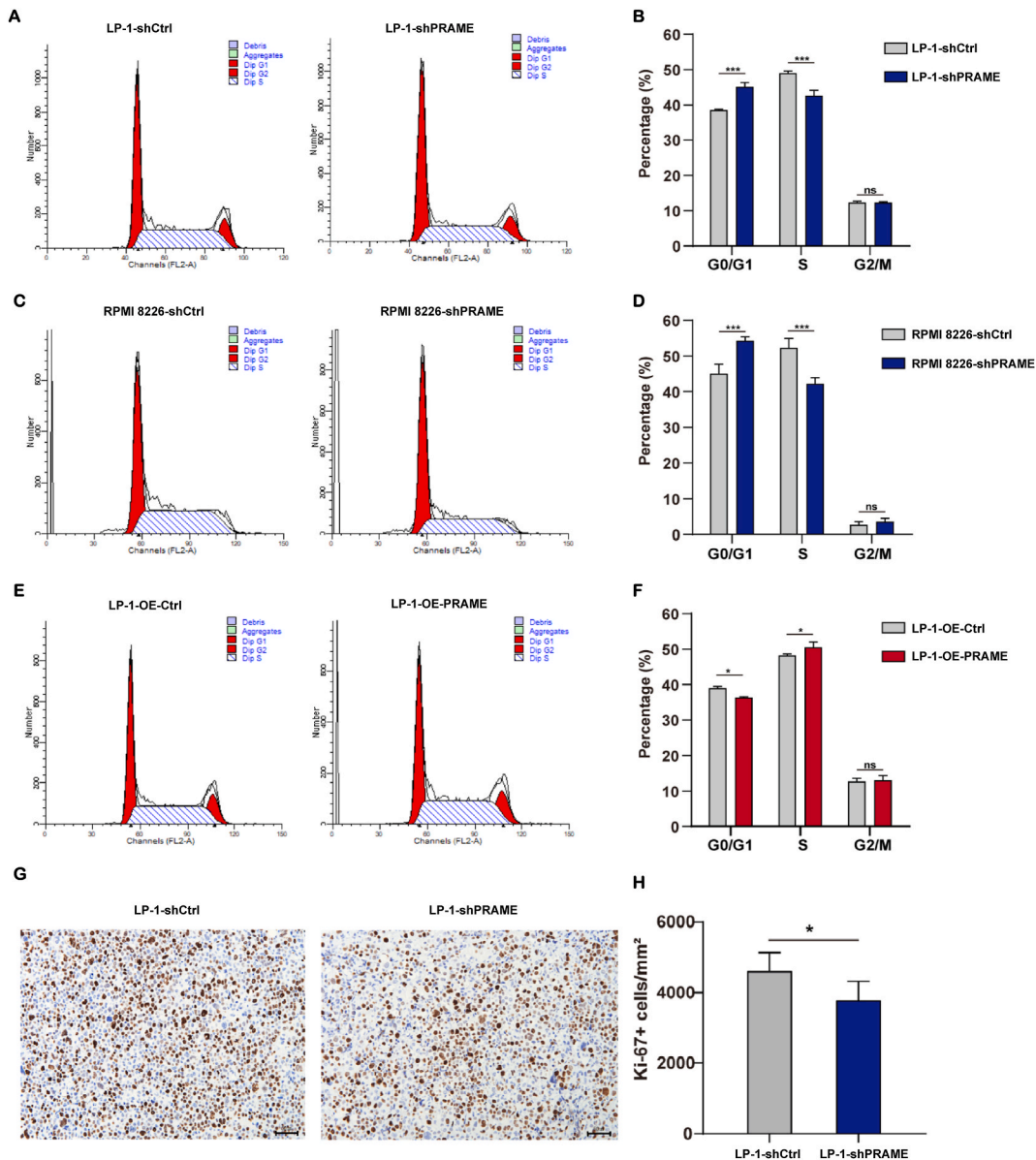
Fig. 3. *PRAME* promotes cell cycle progression in MM cells. (A–F) Cell cycle analysis by flow cytometry in *PRAME* knockdown of (A, B) LP-1 and (C, D) RPMI8226 and overexpression of (E, F) LP-1 cells with corresponding vector controls. (G, H) Ki-67 expression of LP-1-derived xenografts in the *PRAME* knockdown and control groups was tested by immunohistochemistry assay (scale bar, 50 μm). Data are the means ± SD of 3 assays. *ns*, no significance; *$P < 0.05$; **$P < 0.01$; ***$P < 0.001$.
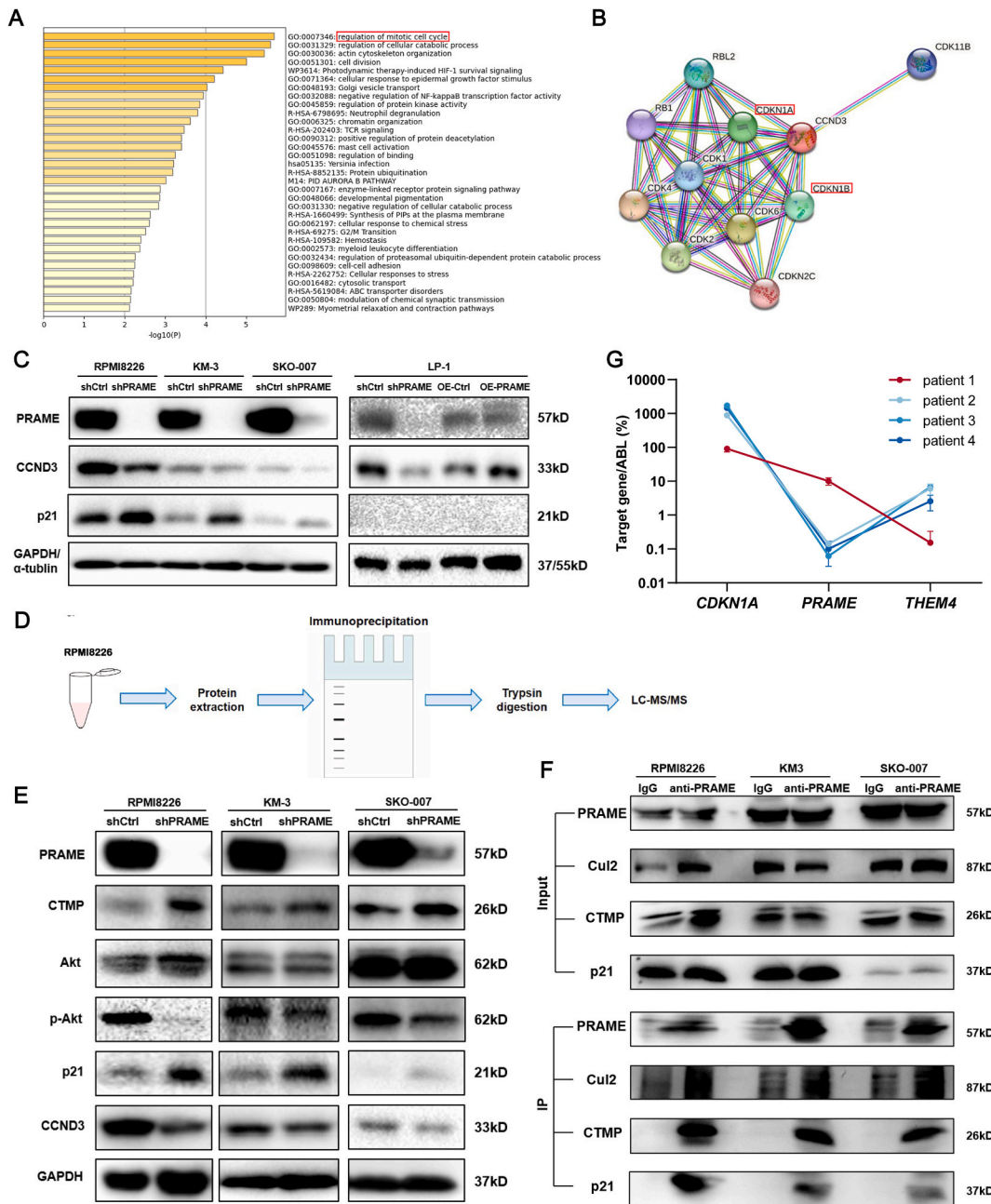
Fig. 4. CTMP and p21 were novel PRAME-interacting proteins in MM cells. (A) Pathway enrichment results based on Metascape analysis of top 100 proteins with reduced expression followed by *PRAME* knockdown. Top 20 pathways were listed. Regulation of mitotic cell cycle was most significantly enriched. (B) Proteins interacting with cyclins analyzed by STRING database. In addition to proteins of cytokinin-dependent kinase (CDK) family, cytokinin-dependent kinase inhibitors (such as *CDKN1A* and *CDKN1B*) are attractive. (C) CCND3 and p21 expression levels tested by Western blot in MM cell lines compared PRAME knockdown or overexpression groups to control groups (related to Fig. S6-Fig. S10). LP-1 was not applied for subsequent protein detection experiments for the low protein expression level of p21 (related to Fig. S11-Fig. S13). (D) Flow diagram of IP-MS of RPMI8226 cells. (E) Western blot verified the CTMP/Akt/p21/CCND3 pathway in MM cell lines RPMI8226, KM-3 and SKO-007 (related to Fig. S14-Fig. S34). Protein expression levels of CTMP and p21 were increased, and *p*-Akt and CCND3 were decreased followed by *PRAME* knockdown. (F) PRAME interacted with CTMP, p21 and Cul2 at the endogenous level. Cells were harvested and subjected to immunoprecipitation with anti-PRAME Ab and immunoblotting with anti-CTMP, anti-p21 and anti-Cul2 Ab (related to Fig. S35-Fig. S42). (G) Higher *PRAME* transcript levels correlated with lower *THEM4* and *CDKN1A* transcript levels in MM patients' plasma cells.

### 3.4. PRAME promotes cell proliferation through CTMP/Akt/p21/CCND3 axis by interacting with CTMP and p21

Proteomic analysis of *PRAME*-knockdown group and the control group of RPMI8226 cells was performed to reveal differentially expressed proteins underlying PRAME related biological effects. Major pathways involved in downregulated proteins were enriched by Metascape analysis [20], and biological process related to mitotic cell cycle regulation was most significantly enriched (Fig. 4A). STRING database was applied for searching cell cycle-related upstream proteins. *CDKN1A* (encoding tumor suppressor p21) and *CDKN1B* (encoding tumor suppressor p27) were the potential candidates (Fig. 4B). Western blot assay confirmed the downregulated expression of cyclin D3 (CCND3) and upregulated expression of p21 in *PRAME*-knockdown RPMI8226, KM-3, SKO-007 and LP-1 cells (Fig. 4C).

IP-MS was further performed to explore PRAME-interacting proteins (Fig. 4D). CTMP was identified as a potential candidate protein. In addition, proteomic analysis indicated that CTMP was upregulated in *PRAME*-knockdown RPMI8226 cells. KEGG pathway database was then used for targeted protein localization. CTMP was found as an upstream binding molecule and inhibitor of Akt. The latter was the key molecule in promoting proliferation and one of the upstream regulators of p21/CCND3. Western blot assay showed that as the expression level of PRAME was knocked down in MM cell lines, CTMP and p21 increased, and *p*-Akt and CCND3 decreased (Fig. 4E). Therefore, PRAME promoted cell proliferation through CTMP/Akt/p21/CCND3 axis.
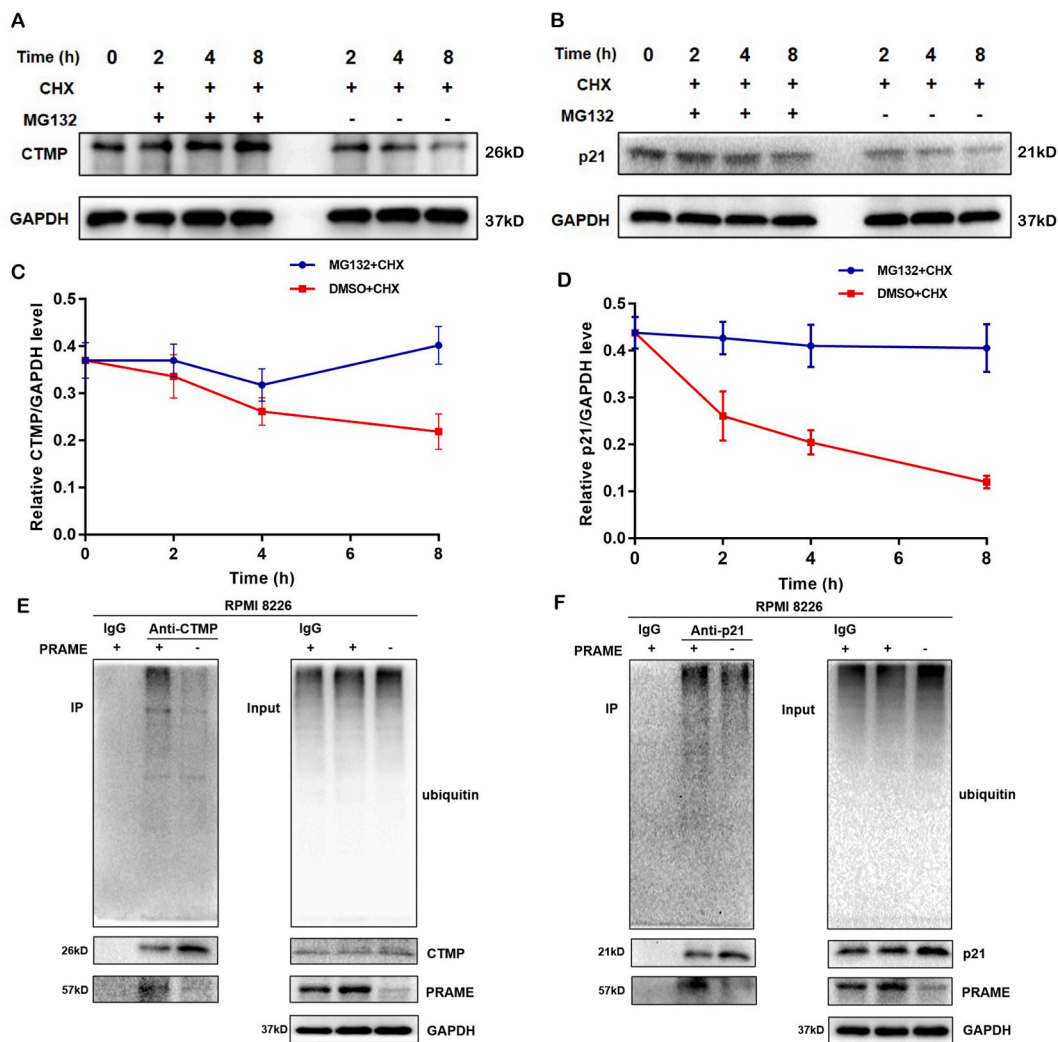
Fig. 5. PRAME degrades CTMP and p21 through UPS. (A, B) CTMP and p21 were degraded by proteasomes. RPMI8226 cells were treated with 10 μmol/L MG-132 versus DMSO in combination with 50 μg/mL CHX for indicated time (0, 2h, 4h and 8h, respectively), and then were subjected to immunoblotting using anti-CTMP and anti-p21 with GAPDH as a loading control (related to Fig. S43-Fig. S46). (C, D) The expression of CTMP and p21 in Fig. 5A and B was quantified by densitometric analysis using ImageJ software, respectively. Data are the means ± SD of 3 assays. *ns*, no significance; *P < 0.05; **P < 0.01; ***P < 0.001. (E, F) PRAME mediated polyubiquitination of CTMP and p21 in RPMI8226 cells. *PRAME* knockdown and control cell models were used. Cells were extracted and subjected to immunoprecipitation with anti-CTMP and anti-p21 Ab and immunoblotting with anti-ubiquitin Ab with MG-132 for 2h and 6h, respectively (related to Fig. S47-Fig. S60).
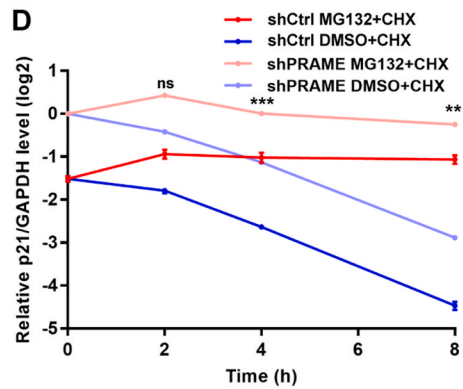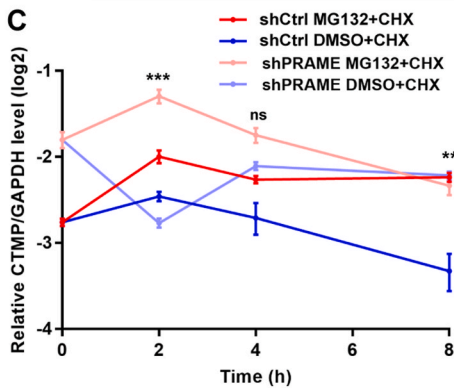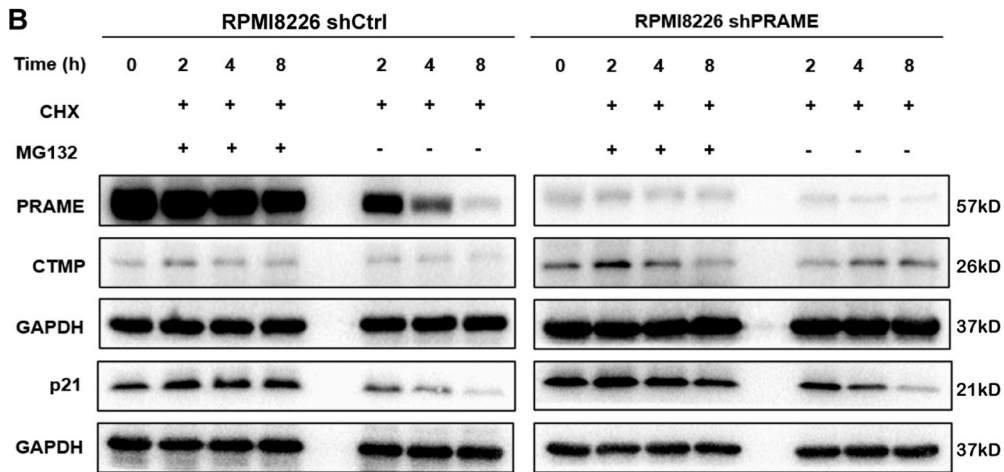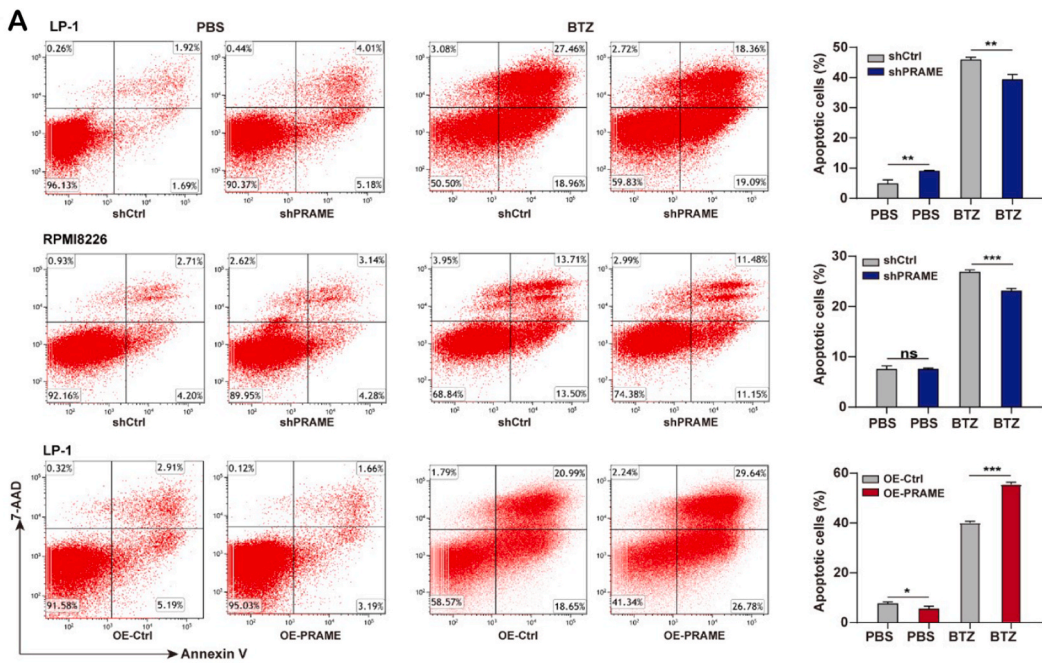
(caption on next page)

Fig. 6. PRAME increases sensitivity of MM cells to bortezomib by targeting CTMP and p21. (A) Apoptosis analysis by flow cytometry in PRAME knockdown and overexpression cells with corresponding vector controls after bortezomib treating for 48h (LP-1, 10 nM; RPMI8226 20 nM). Data are the means ± SD of 3 assays. *ns*, no significance; *$P < 0.05$; **$P < 0.01$; ***$P < 0.001$. (B) CTMP and p21 were degraded more intensely by proteasomes in PRAME high expression group than that in PRAME low expression group. PRAME knockdown and the control RPMI8226 cells were treated with 10 μmol/L MG-132 versus DMSO in combination with 50 μg/mL CHX for indicated time (0, 2h, 4h and 8h, respectively), and then were subjected to immunoblotting using anti-PRAME, anti-CTMP and anti-p21 with GAPDH as a loading control (related to Fig. S61-Fig. S70). (C, D) The expression of CTMP and p21 in Fig. 6B was quantified by densitometric analysis using ImageJ software, respectively. Significance was shown between the fold changes of shCtrl PRAME MG132+CHX/DMSO + CHX group compared to shPRAME MG132+CHX/DMSO + CHX group at each time point. Data are the means ± SD of 3 assays. *ns*, no significance; *$P < 0.05$; **$P < 0.01$; ***$P < 0.001$.

Co-IP (immunoprecipitation with anti-PRAME Ab and immunoblotting with anti-CTMP Ab and anti-p21 Ab, respectively) confirmed the interaction between PRAME and CTMP, and also showed interactions between PRAME and p21 in RPMI8226, KM-3 and SKO-007 cells (Fig. 4F). Meanwhile, immunoprecipitation with anti-CTMP and anti-p21 Ab and immunoblotting with anti-PRAME Ab enriched PRAME in *PRAME* high expression groups, further verifying interactions between CTMP as well as p21 and PRAME (Fig. 5E and F). Therefore, CTMP and p21 were novel PRAME targeting proteins.

We further investigated the correlations between PRAME and its targets using newly diagnosed primary MM patients' BM plasma cells. Quantitative PCR showed that the patient with relatively higher *PRAME* expression showed lower transcript levels of *THEM4* (encoding the protein CTMP) and *CDKN1A* (encoding the protein p21). And those with higher transcript levels of *THEM4* and *CDKN1A* all showed lower *PRAME* expression (Fig. 4G). These data indicated that the interactions between PRAME and CTMP as well as p21 might exist in MM patients' plasma cells.

3.5. PRAME mediates degradation of CTMP and p21 through UPS

Because of the reverse protein levels between PRAME and its interacting proteins CTMP and p21, substrate recognizing role of PRAME related to ubiquitin proteasome mediated protein degradation was speculated in MM. Co-IP results showed the interactions between PRAME and Cul2 (Fig. 4F), which indicated that PRAME might act as a substrate recognizing receptor protein of Cullin RING E3 ligases (CRLs) in the above process. With relatively high expression levels of both CTMP and p21, RPMI8226 cells were used for protein translation blocking and proteasome inhibition assays. Under the premise of protein synthesis blocking, degradation of CTMP and p21 in groups with well-worked proteasomes was obviously increased than that in proteasome inhibited groups (Fig. 5A–D), suggesting that both CTMP and p21 could be degraded by proteasomes in RPMI8226 cells.

In order to further investigate the impact of PRAME on ubiquitination, co-IP assays (Immunoprecipitation individually with anti-CTMP Ab and anti-p21 Ab and immunoblotting with anti-ubiquitin) were conducted. The downregulation of PRAME inhibited the polyubiquitination of CTMP and p21 (Fig. 5E and F). These findings indicated that PRAME functioned as a Cul2-dependent substrate recognizing receptor protein, mediating CTMP and p21 degradation through the ubiquitin-proteasome process.

3.6. PRAME increases bortezomib sensitivity by targeting CTMP and p21

The effect of PRAME expression on the sensitivity of MM cells to bortezomib was investigated. The proportion of apoptotic cells was increased after bortezomib treatment, and *PRAME* knockdown and overexpression individually weakened and enhanced the effect of bortezomib-induced apoptosis (Fig. 6A). These data suggested that *PRAME* expression levels were positively related to bortezomib sensitivity in MM cells.

Protein translation blocking and proteasome inhibition assay were performed to investigate the potential mechanism. Compared with proteasome inhibition group, well-worked proteasomes in the control-*PRAME*-knockdown group degraded CTMP and p21 more intensely than that in the *PRAME*-knockdown group (Fig. 6B–D). Proteasome-mediated degradation of CTMP and p21 was blocked followed by *PRAME* knockdown, revealing that CTMP and p21 degradation showed a *PRAME* expression-level dependent pattern. Interestingly, with well-worked proteasome, *PRAME* knockdown made the level of CTMP even higher than that with proteasome inhibition, indicating that proteasome-mediated CTMP degradation process might be more *PRAME*-dependent than that of p21. Increased proteasome activity followed by high expression of *PRAME* might be one of the reasons for the increased sensitivity to bortezomib.

4. Discussion

In the current study, firstly, we demonstrated that PRAME acted as a tumor promoter in the pathogenesis and progression of MM. Consistent with the results of our previous clinical cohort study [12], this study demonstrated that PRAME promoted proliferation and survival of MM cells *in vitro* and in the xeno-transplant model. These results made it clear for the oncogenic effect of *PRAME* in MM cells.

Several studies have indicated that PRAME conferred growth or survival advantages by binding to the retinoic acid (RA) receptor [21]. Upregulation of PRAME inhibited RA-induced differentiation, growth arrest, and apoptosis in chronic myeloid leukemia (CML) [22]. Another study revealed that *PRAME* overexpression was associated with low expression of apoptosis-inducing genes among pediatric AML patients [23]. The current study elucidated the mechanism of *PRAME* upregulation to promote proliferation from a novel perspective, referring to activation of Akt and its downstream signaling related to cell cycle regulation.

Considering MM is a UPS-dysfunction disease [7], and PRAME functions as an SRS in the ubiquitin proteasome process [15,16], we speculated that PRAME might play its role of substrate recognizing during protein degradation process in MM cells. Based on proteomics and IP combined with MS, PRAME was identified to function as a Cul2-dependent SRS in MM cells, and CTMP and p21 were discovered as PRAME-interacting proteins for the first time. Similar to the present study, Zhang et al. reported PRAME, also acting as a subunit of Cul2-dependent E3 ligase, promoted progression of multiple solid tumors by mediating p14/ARF degradation [24]. These results suggested that PRAME, as an SRS, might widely participate in ubiquitination and degradation process of various proteins in different tumors, but substrates identified by PRAME might be specific among different cell types.

As an inhibitor of cyclin-dependent kinase, p21 (also known as $p21^{WAF1/Cip1}$ or *CDKN1A*) was reported to be regulated by TAAs, and subsequently be degraded through the ubiquitination pathway in several studies. Zhang et al. reported that FBXO22 acted as a subunit of F-box E3 ligase in regulating the ubiquitination and degradation of p21, which promoted the progression of hepatocellular carcinoma [25]. Another study revealed that p21 ubiquitination was blocked by tumor suppressor HERC3 (a member of HERC E3 family) via tumor promotor RPL23A in colorectal cancer [26]. Similarly, in the present study, p21 was also found degraded via the ubiquitination pathway, and thus promoted cell cycle progression of MM cells mediated by the TAA PRAME. These results suggested that p21 might be extensively degraded via ubiquitination process as a TAA-specific substrate of E3 ubiquitin ligases, which might be an important mechanism for tumor progression.

Unlike p21, studies investigating the biological effects of CTMP (carboxyl-terminal modulator protein or thioesterase superfamily member 4, *THEM4*) were still insufficient. As an upstream regulatory molecule of protein kinase B (PKB/Akt), previous studies have revealed high expression of CTMP was the risk factor for ischemic injury and metabolic syndrome [27–29]. Studies focusing on the roles of CTMP in cancers have been increasing in recent years, but results were not fully consistent. CTMP was found to induce apoptosis in several types of solid tumor tissues [30–32], whereas others demonstrated that CTMP acted as an oncogenic driver in breast cancer and head and neck squamous cell carcinoma [33,34]. However, studies exploring the biological roles of CTMP in hematologic malignancies are still lacking, and none of studies have investigated the association between ubiquitination and degradation of CTMP and tumor development. In the current study, we found that CTMP inhibited Akt phosphorylation and functioned as an anti-oncogenic related molecule in MM cells, and first demonstrated that CTMP was degraded by PRAME-mediated ubiquitination, a
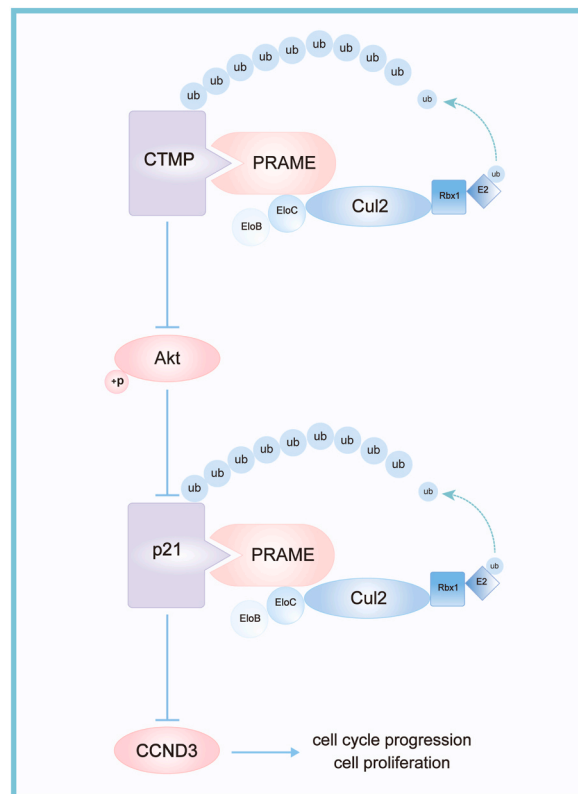
Fig. 7. Mechanism diagram exhibits the role of PRAME in promoting cell proliferation and increasing sensitivity to bortezomib in MM cells. On the CTMP/Akt/p21/CCND3 signal pathway, PRAME plays the role of Cul2-dependent substrate recognizing receptor protein, and interacts with its target CTMP, labeling it with ubiquitin, and making it chemotactic to proteasome and degraded through UPS. The degradation of CTMP contributes to phosphorylation and activation of Akt, which leads to blocking of p21 expression. At the same time, PRAME directly takes p21 as its ubiquitination substrate, directing it degraded through the UPS. Both of the above-mentioned two pathways decrease p21 levels, thus leading to accumulation of CCND3 and promoting the cell cycle progression and cell proliferation.

process associated with tumor progression.

5. Conclusion

The current study revealed that PRAME played a proliferation-promoting role in MM cells. From the perspective of UPS, we demonstrated a novel mechanism by which PRAME promoted MM development through the ubiquitination and degradation of CTMP and p21 (Fig. 7). Remarkably, CTMP and p21 were identified as novel proteins interacting with PRAME. Our findings presented a new insight into understanding the progression of MM and bortezomib treatment resistance, and provided new targets for more precise and effective treatment choices for MM.

Ethics statement

The study was conducted in accordance with the Declaration of Helsinki and was approved by the ethics committee of Peking University People's Hospital [approval number 2018PHC021].

Funding

Data availability

The detailed datasets during the current study are available from the corresponding author on reasonable request.

CRediT authorship contribution statement

Kai Sun: Writing – original draft, Methodology. **Lu Yang:** Writing – original draft, Methodology. **Feng Wang:** Methodology, Data curation. **Ying Liu:** Methodology, Data curation. **Nan Xu:** Methodology. **Zong-Yan Shi:** Methodology. **Wen-Min Chen:** Data curation. **Ke Li:** Validation, Resources. **Ya-Zhen Qin:** Writing – review & editing, Funding acquisition, Conceptualization.

Declaration of competing interest

The authors declare that they have no known competing financial interests or personal relationships that could have appeared to influence the work reported in this paper.

Appendix A. Supplementary data

Supplementary data to this article can be found online at https://doi.org/10.1016/j.heliyon.2024.e34094.

References

[1] H. Ikeda, B. Lethé, F. Lehmann, N. van Baren, J.F. Baurain, C. de Smet, H. Chambost, M. Vitale, A. Moretta, T. Boon, P.G. Coulie, Characterization of an antigen that is recognized on a melanoma showing partial HLA loss by CTL expressing an NK inhibitory receptor, Immunity 6 (1997) 199–208.
[2] Y. Xu, R. Zou, J. Wang, Z.W. Wang, X. Zhu, The role of the cancer testis antigen PRAME in tumorigenesis and immunotherapy in human cancer, Cell Prolif. 53 (2020) e12770.
[3] G. Cazzato, K. Mangialardi, G. Falcicchio, A. Colagrande, G. Ingravallo, F. Arezzo, G. Giliberti, I. Trilli, V. Loizzi, T. Lettini, S. Scarcella, T. Annese, P. Parente, C. Lupo, N. Casatta, E. Maiorano, G. Cormio, L. Resta, D. Ribatti, Preferentially expressed antigen in melanoma (PRAME) and human malignant melanoma: a retrospective study, Genes 13 (2022).
[4] P. Doolan, M. Clynes, S. Kennedy, J.P. Mehta, J. Crown, L. O'Driscoll, Prevalence and prognostic and predictive relevance of PRAME in breast cancer, Breast Cancer Res. Treat. 109 (2008) 359–365.
[5] M.G. Field, C.L. Decatur, S. Kurtenbach, G. Gezgin, P.A. van der Velden, M.J. Jager, K.N. Kozak, J.W. Harbour, PRAME as an independent biomarker for metastasis in uveal melanoma, Clin. Cancer Res. : an official journal of the American Association for Cancer Research 22 (2016) 1234–1242.
[6] K. Partheen, K. Levan, L. Osterberg, G. Horvath, Expression analysis of stage III serous ovarian adenocarcinoma distinguishes a sub-group of survivors, Eur. J. Cancer 42 (2006) 2846–2854.
[7] S.K. Kumar, V. Rajkumar, R.A. Kyle, M. van Duin, P. Sonneveld, M.V. Mateos, F. Gay, K.C. Anderson, Multiple myeloma, Nat. Rev. Dis. Prim. 3 (2017) 17046.
[8] Q.P. Dou, B. Li, Proteasome inhibitors as potential novel anticancer agents, Drug Resist. Updates : reviews and commentaries in antimicrobial and anticancer chemotherapy 2 (1999) 215–223.
[9] J. Adams, The proteasome: a suitable antineoplastic target, Nat. Rev. Cancer 4 (2004) 349–360.
[10] S. Gandolfi, J.P. Laubach, T. Hideshima, D. Chauhan, K.C. Anderson, P.G. Richardson, The proteasome and proteasome inhibitors in multiple myeloma, Cancer Metastasis Rev. 36 (2017) 561–584.
[11] A.J. Cowan, D.J. Green, M. Kwok, S. Lee, D.G. Coffey, L.A. Holmberg, S. Tuazon, A.K. Gopal, E.N. Libby, Diagnosis and management of multiple myeloma: a review, JAMA 327 (2022) 464–477.
[12] Y. Qin, J. Lu, L. Bao, H. Zhu, H. Ji, L. Li, Y. Lai, H. Shi, Y. Wang, Y. Liu, B. Jiang, X. Huang, Bortezomib improves progression-free survival in multiple myeloma patients overexpressing preferentially expressed antigen of melanoma, Chin. Med. J. 127 (2014) 1666–1671.

[13] C. Pellat-Deceunynck, M.P. Mellerin, N. Labarrière, G. Jego, A. Moreau-Aubry, J.L. Harousseau, F. Jotereau, R. Bataille, The cancer germ-line genes MAGE-1, MAGE-3 and PRAME are commonly expressed by human myeloma cells, Eur. J. Immunol. 30 (2000) 803–809.

[14] L. Yang, Y.Z. Wang, H.H. Zhu, Y. Chang, L.D. Li, W.M. Chen, L.Y. Long, Y.H. Zhang, Y.R. Liu, J. Lu, Y.Z. Qin, PRAME gene copy number variation is related to its expression in multiple myeloma, DNA Cell Biol. 36 (2017) 1099–1107.

[15] A. Costessi, N. Mahrour, E. Tijchon, R. Stunnenberg, M.A. Stoel, P.W. Jansen, D. Sela, S. Martin-Brown, M.P. Washburn, L. Florens, J.W. Conaway, R. C. Conaway, H.G. Stunnenberg, The tumour antigen PRAME is a subunit of a Cul2 ubiquitin ligase and associates with active NFY promoters, EMBO J. 30 (2011) 3786–3798.

[16] F.R. Wadelin, J. Fulton, H.M. Collins, N. Tertipis, A. Bottley, K.A. Spriggs, F.H. Falcone, D.M. Heery, PRAME is a golgi-targeted protein that associates with the Elongin BC complex and is upregulated by interferon-gamma and bacterial PAMPs, PLoS One 8 (2013) e58052.

[17] L. Yang, F.T. Dao, Y. Chang, Y.Z. Wang, L.D. Li, W.M. Chen, L.Y. Long, Y.R. Liu, J. Lu, K.Y. Liu, Y.Z. Qin, Both methylation and copy number variation participated in the varied expression of PRAME in multiple myeloma, OncoTargets Ther. 13 (2020) 7545–7553.

[18] J. Zhang, W.Y. Lu, J.M. Zhang, R.Q. Lu, L.X. Wu, Y.Z. Qin, Y.R. Liu, Y.Y. Lai, H. Jiang, Q. Jiang, B. Jiang, L.P. Xu, X.H. Zhang, X.J. Huang, G.R. Ruan, K.Y. Liu, S100A16 suppresses the growth and survival of leukaemia cells and correlates with relapse and relapse free survival in adults with Philadelphia chromosome-negative B-cell acute lymphoblastic leukaemia, Br. J. Haematol. 185 (2019) 836–851.

[19] K. Li, F. Wang, Z.N. Yang, T.T. Zhang, Y.F. Yuan, C.X. Zhao, Z. Yeerjiang, B. Cui, F. Hua, X.X. Lv, X.W. Zhang, J.J. Yu, S.S. Liu, J.M. Yu, S. Shang, Y. Xiao, Z. W. Hu, TRIB3 promotes MYC-associated lymphoma development through suppression of UBE3B-mediated MYC degradation, Nat. Commun. 11 (2020) 6316.

[20] Y. Zhou, B. Zhou, L. Pache, M. Chang, A.H. Khodabakhshi, O. Tanaseichuk, C. Benner, S.K. Chanda, Metascape provides a biologist-oriented resource for the analysis of systems-level datasets, Nat. Commun. 10 (2019) 1523.

[21] M.T. Epping, R. Bernards, A causal role for the human tumor antigen preferentially expressed antigen of melanoma in cancer, Cancer Res. 66 (2006) 10639–10642.

[22] M.T. Epping, L. Wang, M.J. Edel, L. Carlée, M. Hernandez, R. Bernards, The human tumor antigen PRAME is a dominant repressor of retinoic acid receptor signaling, Cell 122 (2005) 835–847.

[23] S. Goellner, D. Steinbach, T. Schenk, G. Bruhn, F. Zintl, E. Ramsay, H.P. Saluz, Childhood acute myelogenous leukaemia: association between PRAME, apoptosis-and MDR-related gene expression, Eur. J. Cancer 42 (2006) 2807–2814.

[24] W. Zhang, L. Li, L. Cai, Y. Liang, J. Xu, Y. Liu, L. Zhou, C. Ding, Y. Zhang, H. Zhao, J. Qin, Z. Shao, W. Wei, L. Jia, Tumor-associated antigen Prame targets tumor suppressor p14/ARF for degradation as the receptor protein of CRL2(Prame) complex, Cell Death Differ. 28 (2021) 1926–1940.

[25] L. Zhang, J. Chen, D. Ning, Q. Liu, C. Wang, Z. Zhang, L. Chu, C. Yu, H.F. Liang, B. Zhang, X. Chen, FBXO22 promotes the development of hepatocellular carcinoma by regulating the ubiquitination and degradation of p21, J. Exp. Clin. Cancer Res. : CRN 38 (2019) 101.

[26] Z. Zhang, Q. Wu, M. Fang, Y. Liu, J. Jiang, Q. Feng, R. Hu, J. Xu, HERC3 directly targets RPL23A for ubiquitination degradation and further regulates Colorectal Cancer proliferation and the cell cycle, Int. J. Biol. Sci. 18 (2022) 3282–3297.

[27] Y. Chen, M. Cai, J. Deng, L. Tian, S. Wang, L. Tong, H. Dong, L. Xiong, Elevated expression of carboxy-terminal modulator protein (CTMP) aggravates brain ischemic injury in diabetic db/db mice, Neurochem. Res. 41 (2016) 2179–2189.

[28] J. Park, Y. Li, S.H. Kim, K.J. Yang, G. Kong, R. Shrestha, Q. Tran, K.A. Park, J. Jeon, G.M. Hur, C.H. Lee, D.H. Kim, J. Park, New players in high fat diet-induced obesity: LETM1 and CTMP, Metab., Clin. Exp. 63 (2014) 318–327.

[29] Q. Zhou, S.E. Leeman, S. Amar, Signaling mechanisms involved in altered function of macrophages from diet-induced obese mice affect immune responses, Proc. Natl. Acad. Sci. U.S.A. 106 (2009) 10740–10745.

[30] C.B. Knobbe, J. Reifenberger, B. Blaschke, G. Reifenberger, Hypermethylation and transcriptional downregulation of the carboxyl-terminal modulator protein gene in glioblastomas, J. Natl. Cancer Inst. 96 (2004) 483–486.

[31] P.O. Simon Jr., J.E. McDunn, H. Kashiwagi, K. Chang, P.S. Goedegebuure, R.S. Hotchkiss, W.G. Hawkins, Targeting AKT with the proapoptotic peptide, TAT-CTMP: a novel strategy for the treatment of human pancreatic adenocarcinoma, Int. J. Cancer 125 (2009) 942–951.

[32] S.K. Hwang, A. Minai-Tehrani, K.N. Yu, S.H. Chang, J.E. Kim, K.H. Lee, J. Park, G.R. Beck Jr., M.H. Cho, Carboxyl-terminal modulator protein induces apoptosis by regulating mitochondrial function in lung cancer cells, Int. J. Oncol. 40 (2012) 1515–1524.

[33] Y.P. Liu, W.C. Liao, L.P. Ger, J.C. Chen, T.I. Hsu, Y.C. Lee, H.T. Chang, Y.C. Chen, Y.H. Jan, K.H. Lee, Y.H. Zeng, M. Hsiao, P.J. Lu, Carboxyl-terminal modulator protein positively regulates Akt phosphorylation and acts as an oncogenic driver in breast cancer, Cancer Res. 73 (2013) 6194–6205.

[34] J.W. Chang, S.N. Jung, J.H. Kim, G.A. Shim, H.S. Park, L. Liu, J.M. Kim, J. Park, B.S. Koo, Carboxyl-terminal modulator protein positively acts as an oncogenic driver in head and neck squamous cell carcinoma via regulating Akt phosphorylation, Sci. Rep. 6 (2016) 28503.